Monte Carlo Fission Source Convergence Diagnosis by Skewness and Kurtosis Estimation Method for Various Benchmark Problems

Seung-Ah Yang * and Ho Jin Park
Department of Nuclear Engineering, Kyung Hee University
#1732 Deogyeong-daero, Giheung-gu, Yongin-si, Gyeonggi-do, 17104, Korea
** Corresponding author: seunga@khu.ac.kr*

1. Introduction

In Monte Carlo (MC) eigenvalue transport calculations, fission source distributions (FSDs) converge by the dominance ratio (DR) which is the convergence rate of an iterative numerical solution. Generally, the DR can be expressed by the ratio of the first higher-order mode eigenvalue of a system to the fundamental eigenvalue, k_1/k_0. For the nuclear system with the high dominance ratio, the MC solutions are very slowly converged. In the slow convergence problems, it is very difficult to ascertain whether the FSD iteration has converged or not. If the FSDs are not fully and sufficiently converged, it can cause its bias. Thus, accurately determining the number of inactive cycles is crucial to obtaining an unbiased Monte Carlo solution.

There are some studies for determining the convergence criteria in MC eigenvalue calculations [1,2]. In the previous studies, we introduced the skewness estimation method (SEM) and kurtosis estimation method (KEM) [3].

In this study, for various benchmark problems - AGN-201K problem [4], 1D Slab problem [5], and two OECD/NEA source slow convergence benchmark problems [6], the SEM and KEM analyses were performed and tested to determine the FSD convergence cycle or the number of inactive cycles in MC eigenvalue calculations.

2. Methods and Results

2.1 Skewness Estimation Method (SEM) and Kurtosis Estimation Method (KEM)

In MC eigenvalue transport calculations, the MC tallies based on a stationary or fully converged FSD should be symmetrically and normally distributed as shown by symmetry and mesokurtic cases. Skewness and kurtosis possess fundamental characteristics that can serve as convergence criteria. Specifically, when the values of Eqs. (1) and (2) fall below a predetermined threshold value, denoted as $\varepsilon_1$and ε_2, they can be used to confirm convergence.

$$\max_m \left|G_1\left[S_m^p, L, N\right]\right| < \varepsilon_1, \quad (1)$$

$$\max_m \left|G_2\left[S_m^p, L, N\right]\right| < \varepsilon_2, \quad (2)$$

$$S_m^p = \int_{V_m} d\boldsymbol{r} S^p(\boldsymbol{r}). \quad (3)$$

where $S^p(\boldsymbol{r})$ is the FSD of neutrons born at any energy, **r**, and cycle index p. Subscript m refers to the cell or region index, and L indicates the minimum cycle length for skewness and kurtosis calculations. $G_1\left[S_m^p, L, N\right]$ and $G_2\left[S_m^p, L, N\right]$indicate the skewness and kurtosis by the distribution of FSDs from the current cycle p to the last cycle N. The two methods were implemented into the McCARD MC transport code [7].

In this study, all the McCARD calculations were conducted on 10,000 cycles (N) with 100,000 neutron histories per cycle and 5 skipped cycles. In the SEM and KEM, the minmum cycle length (L) was set as 4000. The criteria values, ε_1 and ε_2 are 0.5, respectively [8]. In the results, the average skewness and kurtosis were plotted by performing the calculations ten times with a different of initial seeds for the reader's better understanding.

2.2 AGN-201K and 1D Slab Problem

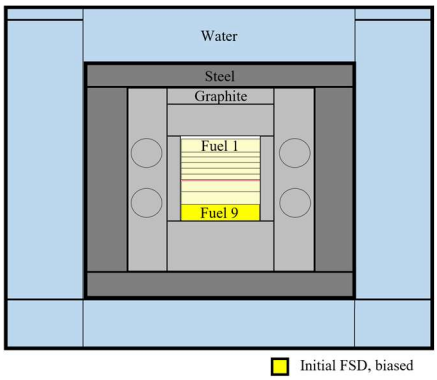

Figure 1. Vertical cross section of AGN-201K

Figure 1 shows the vertical (x-z axis plane) cross section of AGN-201K critical experiment benchmark [4], it has a low DR of about 0.59, which leads to the quick convergence of FSD. In the AGN-201K problem, the initial fission sources are placed at the lowest part among the fuel disks (*Fuel 9*). Nevertheless, as shown in Figs. 2 and 3, the FSDs were converged within the skipped cycles (=5). Figure 4 shows the vertical cross section of the 1D slab test problem with an intermediate DR of 0.9188. Further information on the model's dimensions and results can be found in Reference [5]. In the 1D slab problem, the initial fission sources are positioned towards the left, *CEL 1*. As shown in Figures 5 and 6, the skewness and kurtosis come within the convergence criteria (=0.5) on the 31st and 39th cycle, respectively. Figure 7 demonstrates that the initial guess caused an

imbalance in the FSDs, which gradually converged over cycles.

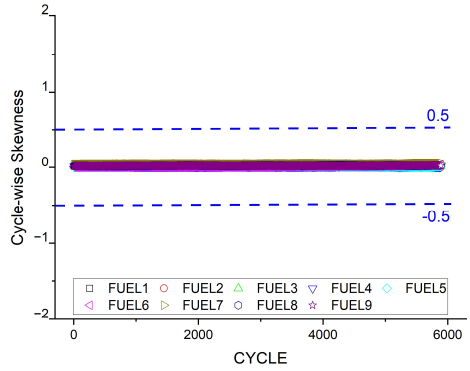

Figure 2. Cycle-wise cumulative skewness of AGN

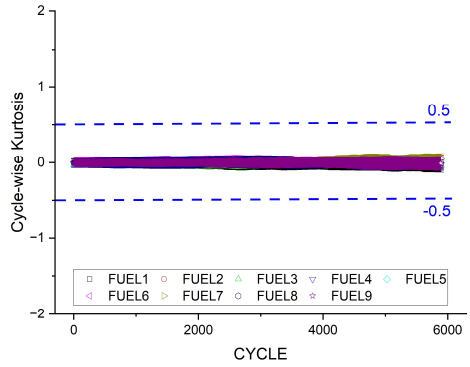

Figure 3. Cycle-wise cumulative kurtosis of AGN

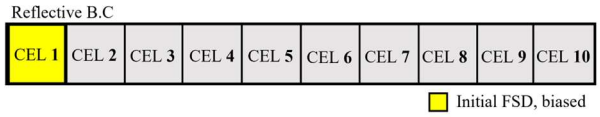

Figure 4. Vertical cross section of slab

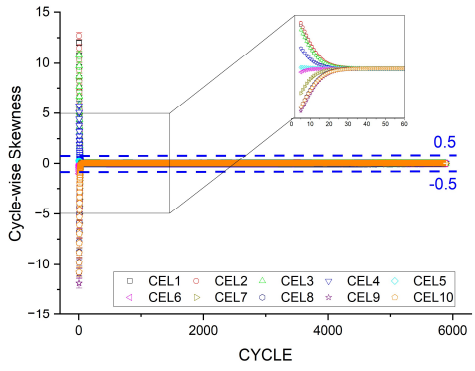

Figure 5. Cycle-wise cumulative skewness of slab

Table I shows the results of convergence cycles by each method. For comparison, the convergence cycle by the Ueki's posterior source convergence diagnosis [1], Shim's on-the-fly stopping criterion (Type A & B) [2] were calculated, additionally. In the 1D slab problem, the number of inactive cycles determined by the Ueki's method was 56, while those by the Shim's types A and B stopping criteria with the default option were 97 and 100. The number of convergence cycles by the SEM and KEM was determined as 31 and 39. It was noted that the convergence cycle by the SEM (ε_1=0.5) and KEM (ε_2=0.5) was similar to the behavior of FSD in Fig. 7, which converges at about 40 cycles.

Table I: Convergence cycle results for the 1D slab problem

Method	Convergence Cycle	
	AGN-201K	SLAB
Ueki's posterior	13	56
Type-A stopping criterion	19	97
Type-B stopping criterion	19	100
SEM	<5	31
KEM	<5	39

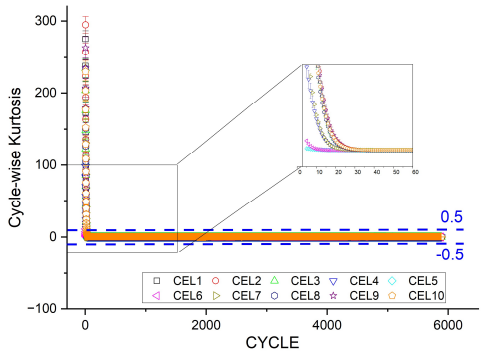

Figure 6. Cycle-wise cumulative kurtosis of slab

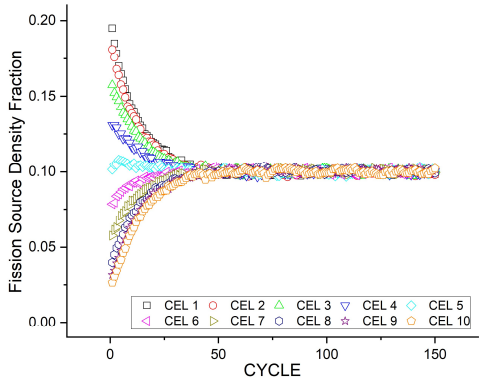

Figure 7. Fission source density fraction of slab

2.3 OECD/NEA Slow Convergence Benchmark Problem

To explore the slow source convergence problem, OECD/NEA expert group on source convergence in criticality safety analysis provided the benchmark problems in the fall of 2000. We selected the two cases among the problems to test the SEM and KEM. One is the checkerboard storage of assemblies (Problem 1) and the other is the pin-cell array with irradiated fuel (Problem 2). For each benchmark problem, the detailed modeling dimensions and results can be found in Reference [6].

2.3.1 Checkerboard storage of assemblies (Problem 1)

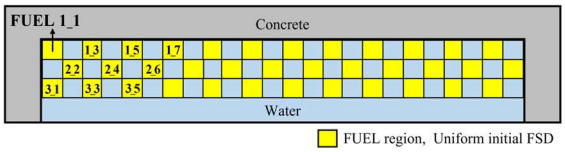

Figure 8. Checkerboard storage of assemblies

The Problem 1 is a fuel storage facility surrounded by concrete on three sides. Fuel and water are stored in an alternating pattern. Problem 1 has a high DR of 0.997. Figure 8 shows the configuration of the checkerboard problem. Because of its asymmetry, the FSDs were converged biased towards the upper-left corner as shown in Fig. 9. In the problem 1, the initial fission sources are uniformly placed at the checkerboard regions.

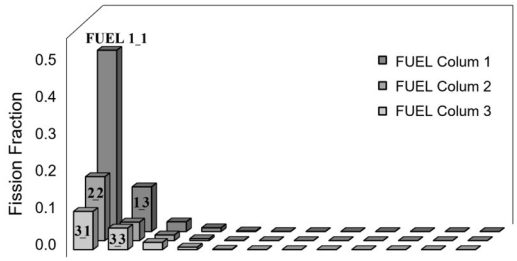

Figure 9. Fission distribution after FSD convergence

Figures 10 and 11 presents the cycle-wise cumulative skewness and kurtosis of Problem 1. The converged cycles were determined by FSDs and its statistics for 10 fuel cells. The number of convergence cycles by the SEM and KEM were determined as 1007 and 1127, respectively. Figure 12 shows the cycle-wise FSDs of Problem 1. Considering the statistical uncertainty and noise, it can be confirmed that the FSDs tend to converge at around 1000 cycles.

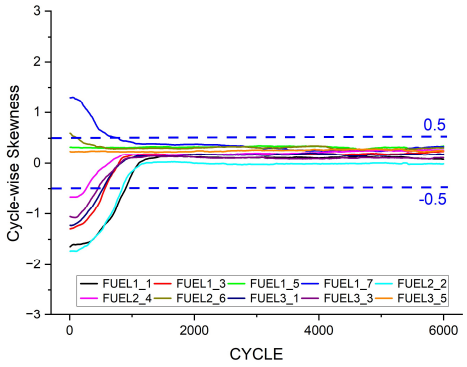

Figure 10. Cycle-wise cumulative skewness of Prob. 1

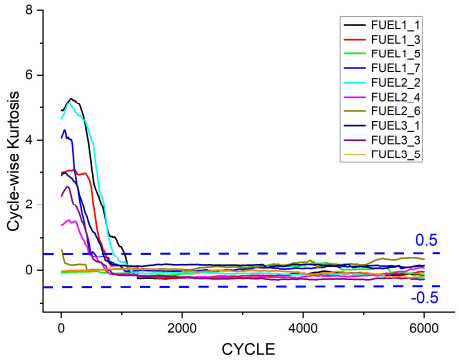

Figure 11. Cycle-wise cumulative kurtosis of Prob. 1

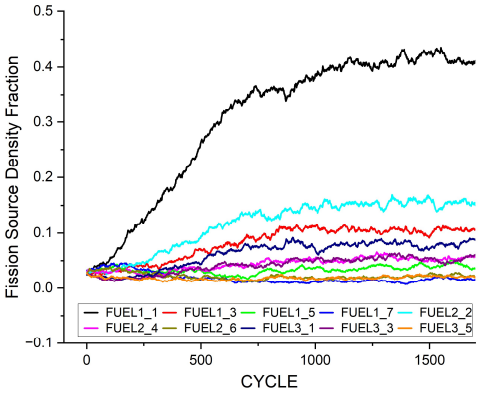

Figure 12. Cycle-wise cumulative FSD fraction of Prob. 1

2.3.2 Pin-cell array with irradiated fuel (Problem 2)

Problem 2 is the light water reactor fuel pin with a non-symmetric idealized burnup distribution in which a lengthy high-burnup, low-multiplication section in the center of the fuel decouples the two multiplying ends as shown in Fig. 13. In this study, we used Case 1-3, which its DR is 0.976, to test the SEM and KEM. In this case, there are higher-enriched uranium on the upper side. Because the FSDs in the lower parts (Fuel 6 ~ Fuel 9) are very small as shown in Figure 14, we used the skewness and kurtosis values from Fuel 1 to Fuel 5. Figures 15 and 16 shows the cycle-wise cumulative skewness and kurtosis of the Problem 2. By the SEM and KEM, the convergence cycle is determined as 752 and 881. Figure 17 shows a slowly changing behavior of FSD and indicates that it converges at about 900 cycles.

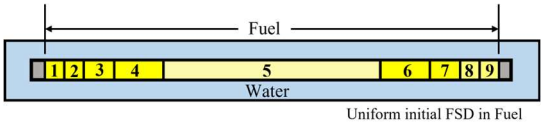

Figure 13. Pin-cell array with irradiated fuel

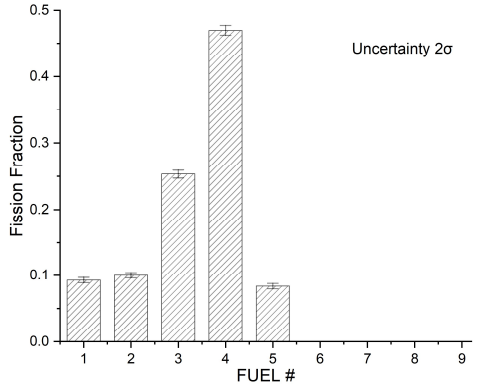

Figure 14. Fission distribution after FSD convergence

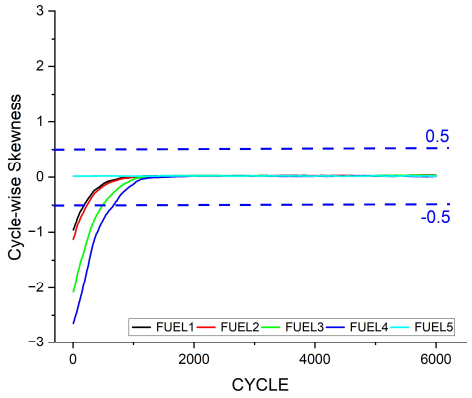

Figure 15. Cycle-wise cumulative skewness of Prob. 2

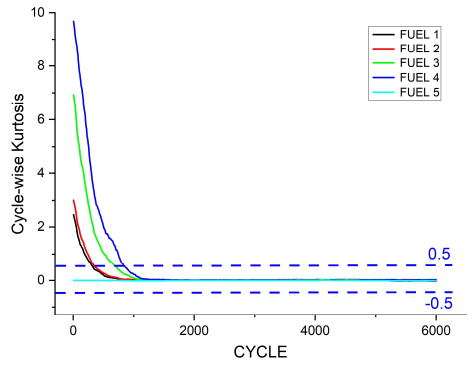

Figure 16. Cycle-wise cumulative kurtosis of Prob. 2

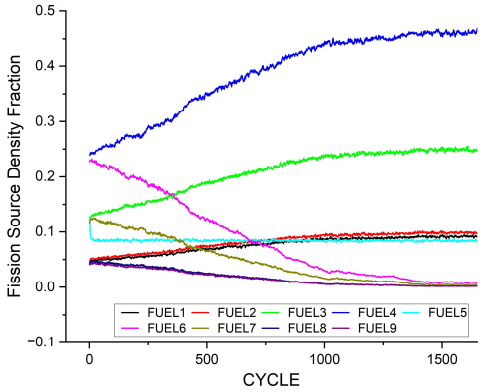

Figure 17. Cycle-wise cumulative FSD fraction of Prob. 2

2.3.3 Summary

Table II shows the results of convergence cycles by each method. For problem 1, the convergence cycle by the SEM (ε_1=0.5) and KEM (ε_2=0.5) was similar to that by the Ueki's posterior source convergence diagnosis and the Shim's type B. In the case of problem 2, it was noted that the SEM and KEM converged at 752nd and 881st cycle, which is the value between Ueki's posterior source convergence diagnosis and the Shim's types A and B stopping criterion. The reference provided the results of the convergence cycles collated and merged from various benchmark participant groups [6] as shown in Table II. Figure 18 shows the Shannon entropy over cycles in the Problems 1 and 2. In comparison to other methods that lead to insufficient inactive cycles or too many inactive cycles, it is observed that the SEM and KEM methods provide more reliable diagnosis of fission source convergence cycle in the Problems 1 and 2.

Table II: Convergence cycle results for OECD/NEA Source Convergence Benchmark

Method	Convergence Cycle	
	Prob. 1	Prob. 2
Reference [6]	700	600
Ueki's posterior	1160	1865
Type-A stopping criterion	163	36
Type-B stopping criterion	1075	48
SEM	1007	752
KEM	1127	881

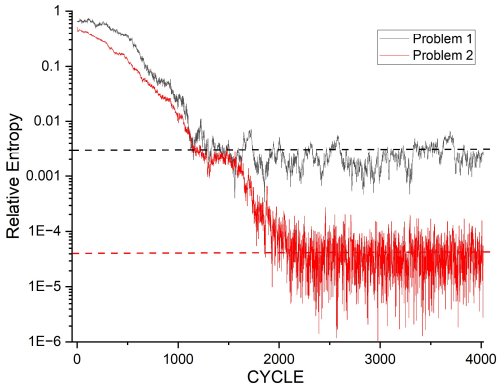

Figure 18. Ueki's posterior source convergence diagnosis

3. Conclusion

The SEM and KEM were applied to OECD/NEA slow convergence benchmark problems as well as low and intermediate DR problems (i.e., AGN-201K and 1D Slab problem) to confirm the performance and reliability of them. From the results, it has been confirmed that the SEM and KEM provided appropriate and effective convergence cycles when considering FSD trends.

In this study, the large neutron histories and long cycle (i.e., 100,000 #/cycle and 10,000 cycles) were applied to the skewness and kurtosis calculations to suppress their statistical fluctuations from the noise of FSDs. In the near future, we will study the modified SEM and KEM that combines Kalman filter to reduce the statistical fluctuation of FSDs.

REFERENCES

[1] T. Ueki, F. B. Brown, Stationarity modelling and informatics-based diagnostics in Monte Carlo criticality calculation, Nucl. Sci. Eng., Vol.149, p. 38, 2005.
[2] H. J. Shim, C. H. Kim, Stopping criteria of inactive cycle Monte Carlo calculations, Nucl. Sci. Eng., Vol.157, p. 132, 2007.
[3] H. J. Park and J. Y. Cho, Skewness and Kurtosis Estimation Method for Fission Source Convergence Diagnosis in Monte Carlo Eigenvalue Calculations, Transactions of the Korean Nuclear Society Spring Meeting Jeju, Korea, July 9-10, 2020.
[4] M. Olguin et al., Investigation of the AGN-201M Research Reactor's Unique Dominance Ratio, Nucl. Sci. Eng, Vol. 196, pp. 1323-1332, 2022.
[5] H. J. Park, H. C. Lee, "Application of Higher Order Fission Matrix for Real Variance Analysis in McCARD Monte Carlo Eigenvalue Calculation," M&C2017, Apr. 16-20, 2017, Jeju, Korea.
[6] R. N. Blomquist, M. Armishaw et al., Source Convergence in Criticality Safety Analyses Phase I: Results for Four Test Problems, Nuclear Science ISBN 92-64-02304-6, OECD 2006 NEA No. 5431.
[7] H. J. Shim et al., "McCARD: Montel Carlo code for advanced reactor design and analysis," Nucl. Eng. Tech., Vol. 44, p.161, 2012.
[8] T. A. Jones, "Skewness and Kurtosis as criteria of normality in observed frequency distributions," Journal of Sedimentary Research, Vol.39, p.1622, 1969.